



Vacuum Polarization Splitting of the Hydrogenic M-shell and Muon Dynamics
in Catalyzed Fusion

M. Jändel ¹⁾, S.E. Jones ²⁾, B. Müller ^{1,3)} and J. Rafelski ^{1,4)}

CERN - Geneva

Abstract

We consider the dynamics of the muonic deexcitation cascade in deuterium and tritium targets used in muon catalyzed fusion research. We find a profound influence of the vacuum polarization splitting of the hydrogenic M-shell on the muonic cascade. Furthermore, the cascade depends sensitively on the suppression of transfer processes between certain excited muonic deuterium and tritium atoms. Our results agree with recent experiments by S.E. Jones et al. where a much greater population of the ($d\mu$) 1s-state was found than previously predicted.

-
- 1) CERN, CH- 1211 Geneva 23
 - 2) Dept of Physics and Astronomy, Brigham Young University, Provo, UT 84602
 - 3) Institut für Theoretische Physik, J.W.Goethe-Universität, Postfach 11 19 32, D-6000 Frankfurt
 - 4) Department of Physics, University of Arizona, Tucson, AZ 85721

1. Introduction

Understanding of the atomic capture and hydrogenic deexcitation cascade of muons is of profound importance in the study of muon catalyzed fusion of hydrogen isotopes [1] [2] [3]. In the case of muons entering a deuterium-tritium fusion vessel, the fraction of muons reaching the deuterium ground state has a large influence on the overall fusion rate [4]. By understanding the muonic cascade one can possibly create conditions favourable for muon transfer to tritium before the ground state is reached.

The muonic cascade is determined by a competition between radiative transitions, density dependent external Auger transitions, density and temperature dependent quenching of the sublevels in muonic atoms and transfer processes which depend both on density and tritium concentration. As the rates for these processes differ widely between states within a given principal shell, the cascade can take a very different route depending on the actual population of these substates. The original theoretical model of Menshikov and Ponomarev [4] has been found to differ from the experimental results and we have therefore reviewed the entire subject matter anew. Even though our approach is parallel to that of Ref. 4 we arrive at entirely different results. This occurs as a consequence of a) the suppression of some transfer processes because of molecular phenomena and b) inclusion of the vacuum polarization splitting of the M-shell.

For states in the M-shell and higher, Stark mixing is believed to be sufficiently fast so that the substates of a principal shell are populated statistically, for densities not less than $\Phi=0.01$ (in units of the liquid hydrogen density 4.25×10^{22} atoms/cm³) [5]. However, this does not imply

that the relative population of the states is determined solely by their quantum statistical weight, i.e. their degeneracy factor as Menshikov and Ponomarev have assumed [4]. The relative populations also depend sensitively on the energy splittings within the shell states if these happen to lie in a range comparable to the characteristic thermal energy kT . A detailed study of (μd) elastic and charge-exchange cross sections by Menshikov and Ponomarev [6] shows that the thermalization rate of excited muonic atoms is 10^{12} s^{-1} at $\Phi=1$ which is one order of magnitude larger than the Auger decay rates of M-shell states. Radiative transition rates are about 10^{10} s^{-1} for $n > 2$ and will hence not cause any significant deviation from a thermal distribution for densities larger than $\Phi = 10^{-2}$. Neglecting first for simplicity the splitting within the 3p and 3d fine and hyperfine structure states, the populations n_{3s} , n_{3p} and n_{3d} are related by,

$$\begin{aligned} n_{3p} &= 3n_{3s} \exp(-\Delta_{3p}/T) \\ (1) \quad n_{3d} &= 5n_{3s} \exp(-\Delta_{3d}/T) \end{aligned}$$

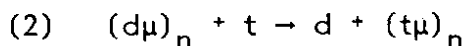
where Δ_{3p} and Δ_{3d} are the energy differences to the 3s state, respectively, and T is the temperature. The dominant source of M-shell splitting is vacuum polarization, contributing 66.5 meV to the $\Delta_{3p} = 69$ meV energy difference between the $3s_{1/2}$ and $3p_{3/2}$ states in muonic deuterium with the s-states being more bound [7]. Since this splitting influences the statistical populations up to $T \sim 700\text{K}$, there will be significant temperature dependence of the muonic cascade in deuterium which in turn influences the kinetics of the muon catalysis cycle as we shall demonstrate in Section 2. We will further show in Section 3 that an important test of the present ideas is obtained by measurement of the temperature and density dependence of K_α , K_β and L_α yields in pure deuterium.

The thermal equilibrium will not prevail in the more strongly split L-shell, since the rate of quenching at $T < 500\text{K}$ is smaller than the rate of deexcitation of the 2p-level. The presence of resonant quenching in atomic targets [8] suggests that further important effects could show up at still higher temperatures.

2. 1s-population of muonic deuterium in D-T mixture

The relevant level structure and decay scheme of a μd atom is shown in Fig.1. Level splittings in the L- and M-shell are mainly determined by vacuum polarization corrections, which amount to a relative shift of 229 meV between the 2s and 2p states, and 66.5 meV and 72.1 meV between the 3s and 3p and the 3s and 3d states, respectively. The values used in our calculations [7] (see the Table) include also fine structure and hyperfine structure effects which, however, are much smaller. The strengths of the radiative and (external) Auger transitions and of the transfer rates [4] are shown in Fig. 1, in units of 10^{11} s^{-1} . The Auger and transfer rates depend linearly on the target density Φ . We note the competition between Auger and radiative transitions of the 3p state, with the radiative decay into the 1s ground state dominating at lower densities ($\Phi < 0.5$).

The rates for the transfer process



have been calculated [4] for collisions of $\text{d}\mu$ atoms with tritium atoms, not molecules. For atom-molecule collisions the transfer is expected [9] to be strongly suppressed due to absence of final states, if the released energy is not much larger than the molecular dissociation energy (about 4.6 eV). Since the difference in binding energy of $\text{t}\mu$ and $\text{d}\mu$ is $48\text{eV}/n^2$ in the n-th

principal shell, we find that the transfer rate should be much less than the predicted atomic rate for all shells with $n > 2$. We have therefore scaled these rates by an adjustable factor x which should be much smaller than unity for a completely molecular target. It is quite conceivable that under usual experimental conditions the transfer rate for $n > 2$ levels is effectively zero, a fact which can explain the disagreement between the previously calculated [4] $(d\mu)_{1S}$ population and experiment [10]. The factor x can then be interpreted as the fraction of all tritium atoms that are not bound in molecules.

We now turn to consider the consequences for muon catalyzed fusion. If the muon reaches the $1s$ -state in deuterium the $(d\mu)$ fusion cycle is significantly delayed due to the very low transfer rate ($3 \times 10^8 \text{ s}^{-1} \Phi C_t$) from this state. The $(d\mu)$ K-shell population probability is, therefore, a quantity of considerable practical interest. This probability can be written $C_d q_{1S}$ where q_{1S} is the probability for a muon, initially captured by a deuteron, to reach the $(d\mu)$ groundstate. C_d is the fraction of deuterium in the target. Calculations by Menshikov and Ponomarev [4], which are based on uninhibited transfer from all excited states and ignore the splitting of the M-shell, predict very small values for q_{1S} at $\Phi=1$. Experiments specifically designed to measure q_{1S} have been carried out recently [11] as the analysis of catalyzed fusion dynamics has not been consistent [10] with the small q_{1S} values obtained by Menshikov and Ponomarev [4].

Molecular suppression of final states is expected [9] to inhibit strongly transfer from states above the $d\mu$ L-shell. Our results for $q_{1S}(C_t)$, assuming transfer suppression to molecular targets ($x=0$) and thermal distribution in the M-shell, are shown in Fig. 2a for several densities (C_t is the fraction of tritium, $C_d + C_t = 1$). They yield much larger values, e.g. $q_{1S} \approx 0.5$ at $\Phi=1$ and $C_t=0.5$ as compared with $q_{1S} \approx 0.08$ predicted by Menshikov and Ponomarev [4]. We also find a Φ -dependence in better agreement

with experiment. The dependence on C_t was experimentally measured by Jones et al. [10] for $\Phi=0.72$ and $T=300\text{K}$, who found $q_{1S}(C_t=0.5)/q_{1S}(C_t=0.04) = 0.72 \pm 0.15$ (assuming constant λ_{dt}). Our result for this ratio is 0.67, whereas Menshikov and Ponomarev find the much smaller value of 0.14. The measured Φ dependence [10] at $C_t=0.5$ and $T=300\text{K}$ is $q_{1S}(\Phi=0.72)/q_{1S}(\Phi=0.12) = 0.98 \pm 0.35$. The corresponding theoretical results are 0.65 in our model and 0.46 in the Menshikov-Ponomarev model.

The dependence of q_{1S} on the reduced strength of the transfer from higher states is investigated in Fig.2b, which shows q_{1S} as function of C_t for several values of the parameter x denoting the fraction of tritium atoms that are not bound in molecules. Our calculation with the value $x=1$ corresponds to Ponomarev's model, but includes the effects of vacuum polarization on the populations of the L- and M-shell substates. An increasing fraction (x) of atomic tritium clearly leads to a significant reduction in the value of q_{1S} , as expected [9].

The temperature dependence of q_{1S} is a sensitive probe for the value of x . In Fig. 3 we show that q_{1S} decreases with increasing temperature for $x=0$ while this trend is reversed even for $x = 0.01$. In the Menshikov-Ponomarev model ($x = 1$), modified to include a thermal distribution of M-shell sublevels, q_{1S} increases by more than a factor three within the interval $T = 0 - 500$ K. The original Menshikov-Ponomarev model has no temperature dependence. Using data of S.E. Jones et al. [10] for λ_{dt} and q_{1S} , and assuming that λ_{dt} is independent of temperature, we find that q_{1S}^{-1} is proportional to $(1 + 6 \pm 1 \times 10^{-4}T)$. This result is displayed in Fig. 3 and is in reasonable agreement with the $x = 0$ case (i.e. the absence of atomic tritium and suppression of transfer from $n>2$ ($d\mu$) atoms to molecular tritium).

Let us briefly return to the kinetics of muon catalyzed fusion to illustrate the influence of the $(\mu d)_{1S}$ population on the efficiency of the catalyzed fusion process. The normalized fusion rate λ_c can be written

$$(3) \quad \lambda_c^{-1} = \frac{C_d q_{1S}}{C_t \lambda_{dt}} + \frac{1}{C_d \lambda_{dt\mu}}$$

where $\lambda_{dt\mu}$ is the molecule formation rate. Taking typical measured values: $\lambda_{dt} = 3 \times 10^8 \text{ s}^{-1}$ and $\lambda_{dt\mu} = 6 \times 10^8 \text{ s}^{-1}$ at $C_t = C_d = 0.5$ we find that $\lambda_c \sim (q_{1S} + 1)^{-1}$. In Fig. 2b we obtain $q_{1S} = 0.5$ for $\Phi=1$, $C_t=0.5$ and $x=0$. The importance of the value of q_{1S} increases as the molecule formation rate increases. For large $\lambda_{dt\mu}$ we get $\lambda_c \sim q_{1S}^{-1}$. Using Fig. 2b we note that $q_{1S} \approx 0.5 - 10x$ at $\Phi=1$ for a small atomic tritium fraction x . Increasing x to 1% would hence, for large $\lambda_{dt\mu}$, lead to a 20% increase of the cycle rate.

3. Muonic X-rays in pure deuterium

Let us now discuss the muonic cascade in pure deuterium which can be employed to verify the T dependence in the M-shell population. In detail, after being captured in higher states, the muon cascades down mainly by Auger processes until it reaches the M-shell ($n=3$). For not too low densities ($\Phi > 0.1$), we assume that the population of the substates of the M-shell is thermally equilibrated. Due to continuous fast repopulation of all states within the shell the independent populations n_{3s} , n_{3p} , and n_{3d} decay with the same rate even though the likelihood of finding the muon in one of the states is subject to the probability distribution eq. (1) (ignoring fine and hyperfine structure effects).

However, only muons populating the 3p state contribute to the yield of K_β ($3p \rightarrow 1s$) radiation. This yield is hence directly proportional to the 3p partial population and the branching ratio into this radiative channel. De-

decays from both the 3s and 3d states populate the 2p level which also decays into the 1s level. Taking the ratio of the K_β and prompt K_α radiation (Fig. 4a) we eliminate to a large extent our ignorance about other details in the cascade and concentrate only on some of the transitions shown in Fig. 2. Fig. 4a shows as a function of T for different Φ the ratio K_β/K_α . In particular, we note the strong dependence on the precise splitting between the 3p and 3s states indicating the sensitivity of this quantity to the hypothesis of thermal equilibrium in the M-shell. The temperature dependence shown in Fig. 4a provides therefore a measure of the energy difference between the 3p and 3d states and is hence an indirect measurement of the vacuum polarization effect.

Further information about the muonic cascade could be obtained from a measurement of the relative yields of K_β (3p \rightarrow 1s) and L_α (all 3 \rightarrow 2) radiation as a function of temperature; see Fig. 4b. According to our hypothesis of thermal distribution, the 3s-state is predominantly occupied at low temperature. The expected yield ratio (see Fig. 4b) has a characteristic temperature dependence in the vicinity of $T \approx 0.2 \times \Delta_{3p} \approx 150\text{K}$, which is

$$(4) \quad Y(L_\alpha)/Y(K_\beta) = 0.012 \exp(\Delta_{3p}/T) + 0.133 + 0.65 \exp((\Delta_{3p} - \Delta_{3d})/T)$$

In summary, the temperature dependence of the M-shell sublevel populations can be probed by the observation of relative yields of K_α , K_β and L_α radiation in muonic deuterium. The effect of thermal spikes [12] caused by energy deposition from stopped muons would be observed as an enhanced effective temperature. Clearly, no variation will be seen in the relative yields should the partial populations be independent of temperature.

4. Conclusions

We have improved the understanding of the muon cascade and muon dynamics in a mixture of deuterium and tritium, and have found a significant temperature dependence of q_{1S} due to the vacuum polarization splitting in the M-shell of the (μd) -atom. Together with the suppression of certain transfer rates of muons from deuterium to tritium, this leads to a better description of recent experimental results [10].

In view of our improved understanding of the muon dynamics it is apparent that in order to maximize the number of fusions a muon can catalyze before it decays, we must bring about either that the 2s-state in $(d\mu)$ is predominantly populated leading to a fast transfer to tritium or that this transfer occurs even earlier [9], should atomic tritium be a significant component in the target. Moreover we predict that by increasing the fraction of free tritium atoms, one will increase the cycle rate leading to a significantly increased fusion yield.

Table 1:

Energies of the hyperfine structure states in the L- and M-shell of muonic deuterium, measured with respect to the $L=1, J=F=1/2$ state [7].

(L_J)	F	$E_{n=2}$ (meV)	$E_{n=3}$ (meV)
$s_{1/2}$	1/2	0	0
	3/2	3.07	1.00
$p_{1/2}$	1/2	230.67	66.91
	3/2	231.69	67.21
$p_{3/2}$	1/2	239.87	69.63
	3/2	240.08	69.69
	5/2	240.42	69.79
$d_{3/2}$	1/2	---	75.32
	3/2	---	75.36
	5/2	---	75.42
$d_{5/2}$	3/2	---	76.22
	5/2	---	76.25
	7/2	---	76.28

References

- [1] L.Bracci and G.Fiorentini, Phys. Rep. 86, 169 (1982).
- [2] J. Rafelski and S.E Jones, Sci. Am. 255, July (1987) p. 84.
- [3] S.E. Jones, Nature, 321, 127 (1985).
- [4] L.I.Menshikov and L.I.Ponomarev, Pis'ma Zh. Eksp. Teor. Fiz. 39, 542 (1984) (JETP Lett. 39, 663 (1984)).
- [5] L.Bracci and G.Fiorentini, Nucl. Phys. A364, 383 (1981).
- [6] L.I. Menshikov and L.I. Ponomarev, Z. Phys. D2, 1 (1986).
- [7] E. Zavattini, private communication. We thank Dr. Zavattini for communication of unpublished detailed calculations.
- [8] J.S. Cohen and J.N. Bardsley, Phys. Rev. A23 , 46 (1981).
- [9] S.E.Jones and J.Rafelski, Internal report and patent application, Brigham Young University.
- [10] S.E. Jones et al., Phys. Rev. Lett. 56, 588 (1986).
- [11] M. Leon, contribution to Proc. of Int. Symp. on Muon Catalyzed Fusion, Leningrad May 26-29 (1987).
- [12] M. Jändel, CERN-TH 4832/87 (1987).

FIGURE CAPTIONS

Figure 1. Level scheme of muonic deuterium (tritium). The transition rates are shown in units of 10^{11} s^{-1} , the density Φ is normalized to liquid hydrogen density ($4.25 \times 10^{22} \text{ cm}^{-3}$). C_t is the tritium concentration, x is the scaling factor explained in the text. Dashed and solid lines denote radiative and Auger transitions respectively.

Figure 2(a) Normalized fraction q_{1S} of muons reaching the deuterium 1s-state, as a function of tritium concentration at $T=0$ for various densities. The density Φ is in units of liquid hydrogen density. (b) Same as (a), but for various values of the scale factor x , which denotes the strength of transfer from states above the L-shell (e.g. due to a presence of an atomic tritium fraction x). The density is $\Phi=1$ (LHD). The temperature dependence is significant, on the scale of the figures, only for $x > 0.1$.

Figure 3. Temperature dependence of q_{1S} for various tritium concentrations C_t and atomic tritium fractions x (solid lines). The "observed" temperature dependence is extracted from data in Ref. 10 assuming that λ_{dt} is independent of temperature. The shaded area around the dashed line shows experimental errors. The density is $\Phi=1$.

Figure 4 (a). Ratio of the yields of K_β and K_α radiation in pure deuterium as a function of temperature for various densities. Dashed lines show the effect of changing the 3s-3p splitting ΔE_{3p} by $\pm 10 \text{ meV}$ for $\Phi=0.01$. (b) Same as (a) but for the density independent ratio of the yields K_β and L_α .

DECAY OF MUONIC DEUTERIUM AND MUON TRANSFER TO TRITIUM

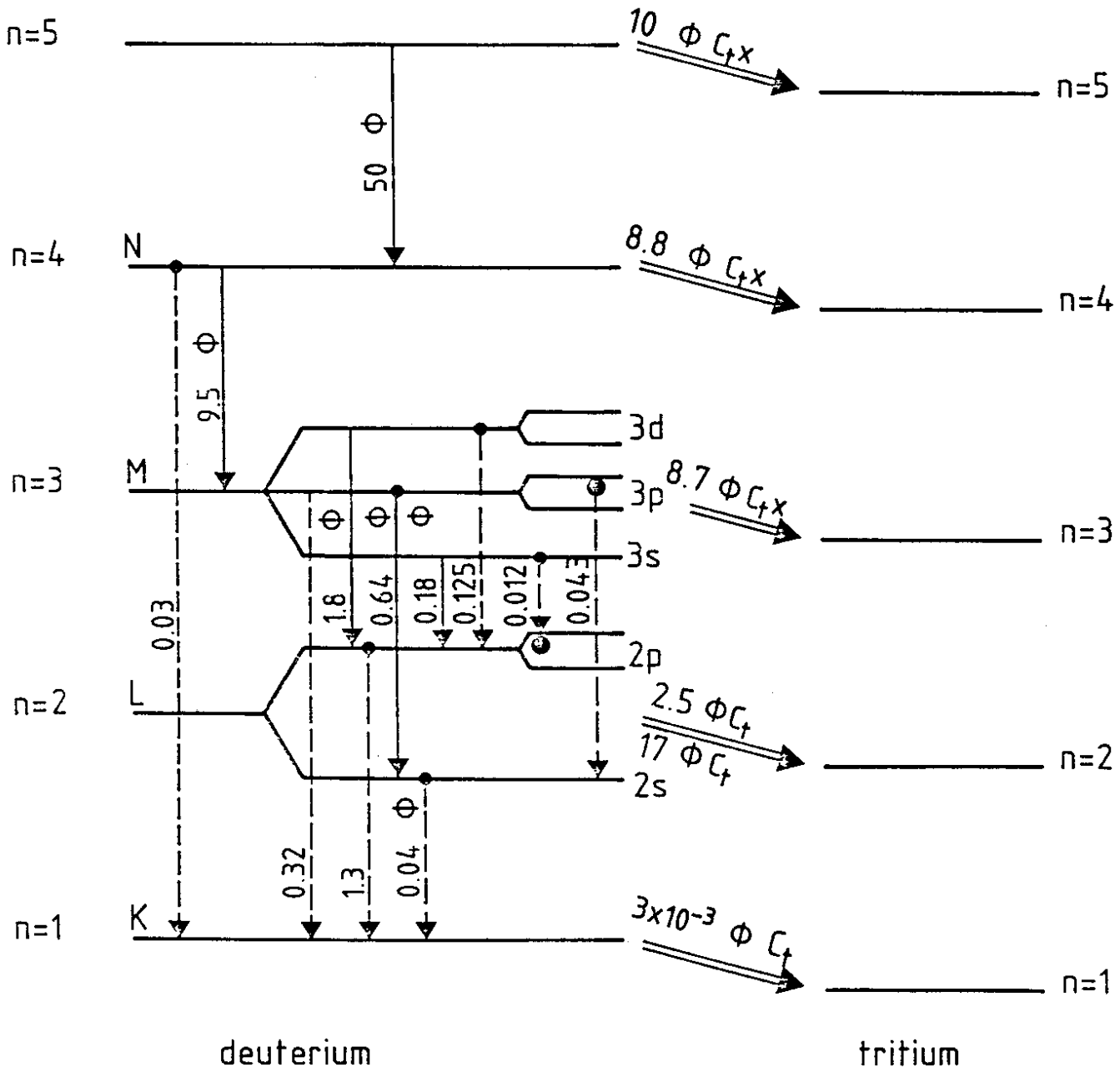


FIG. 1.

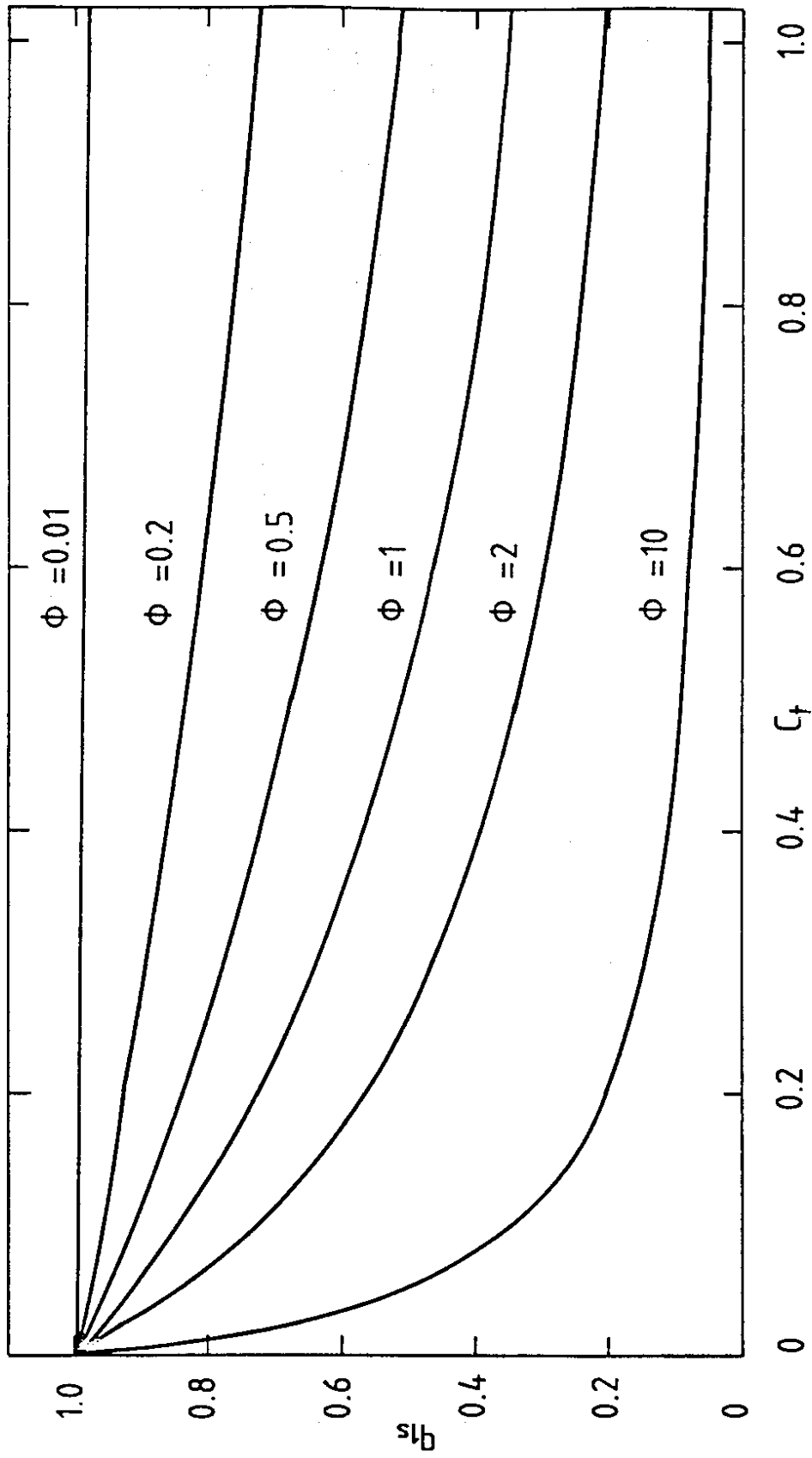


FIG. 2(a).

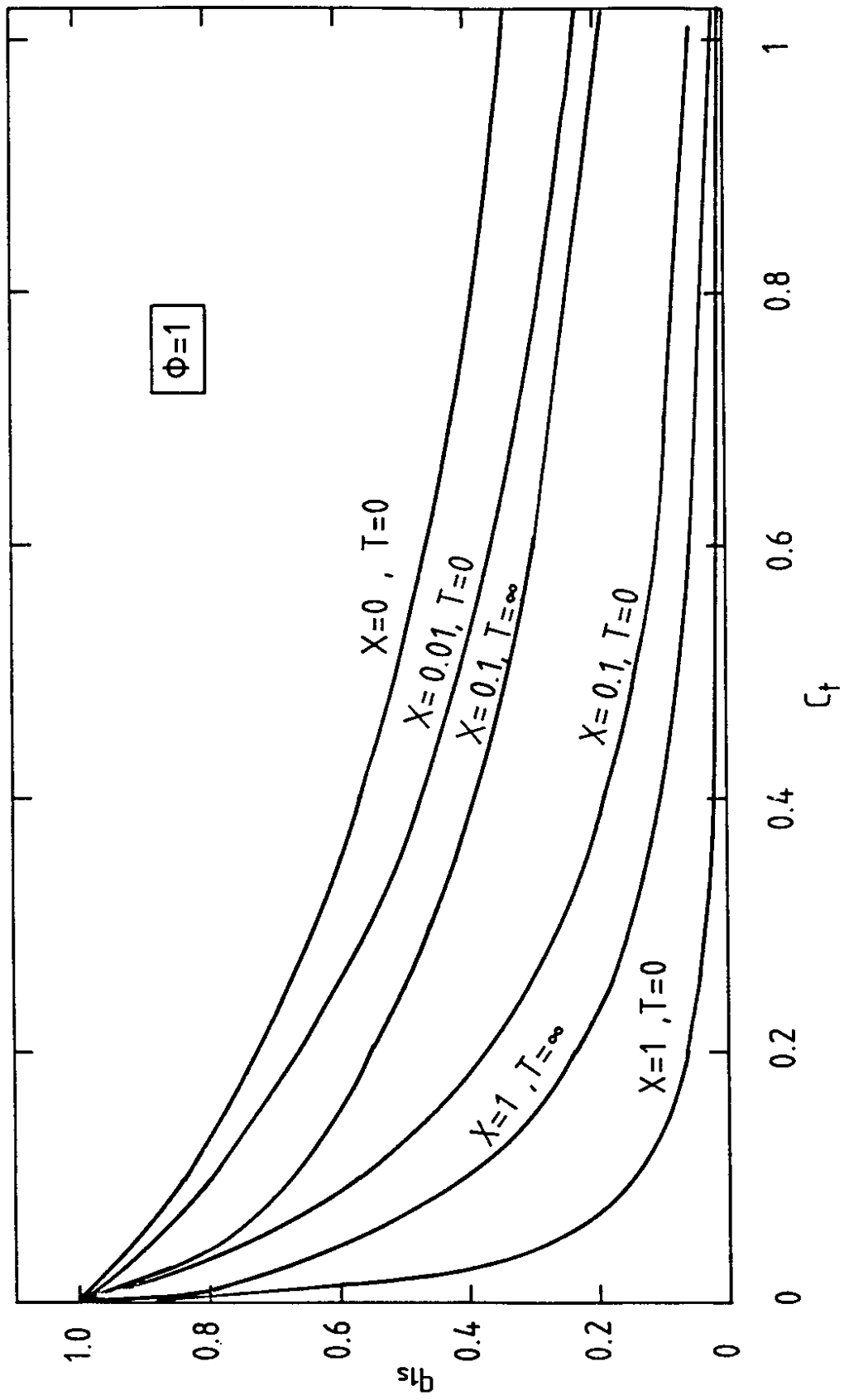


FIG. 2(b)

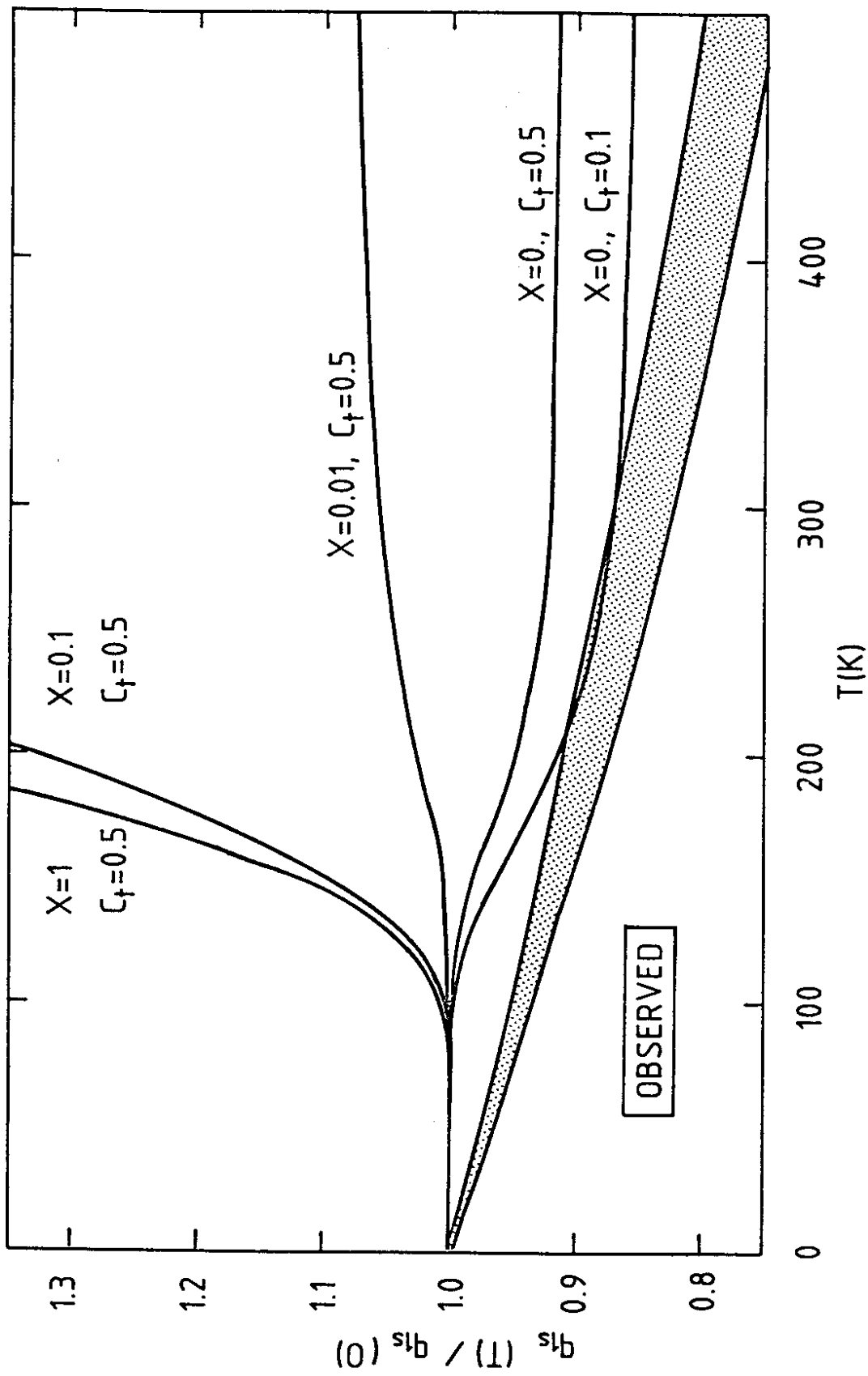


FIG. 3.

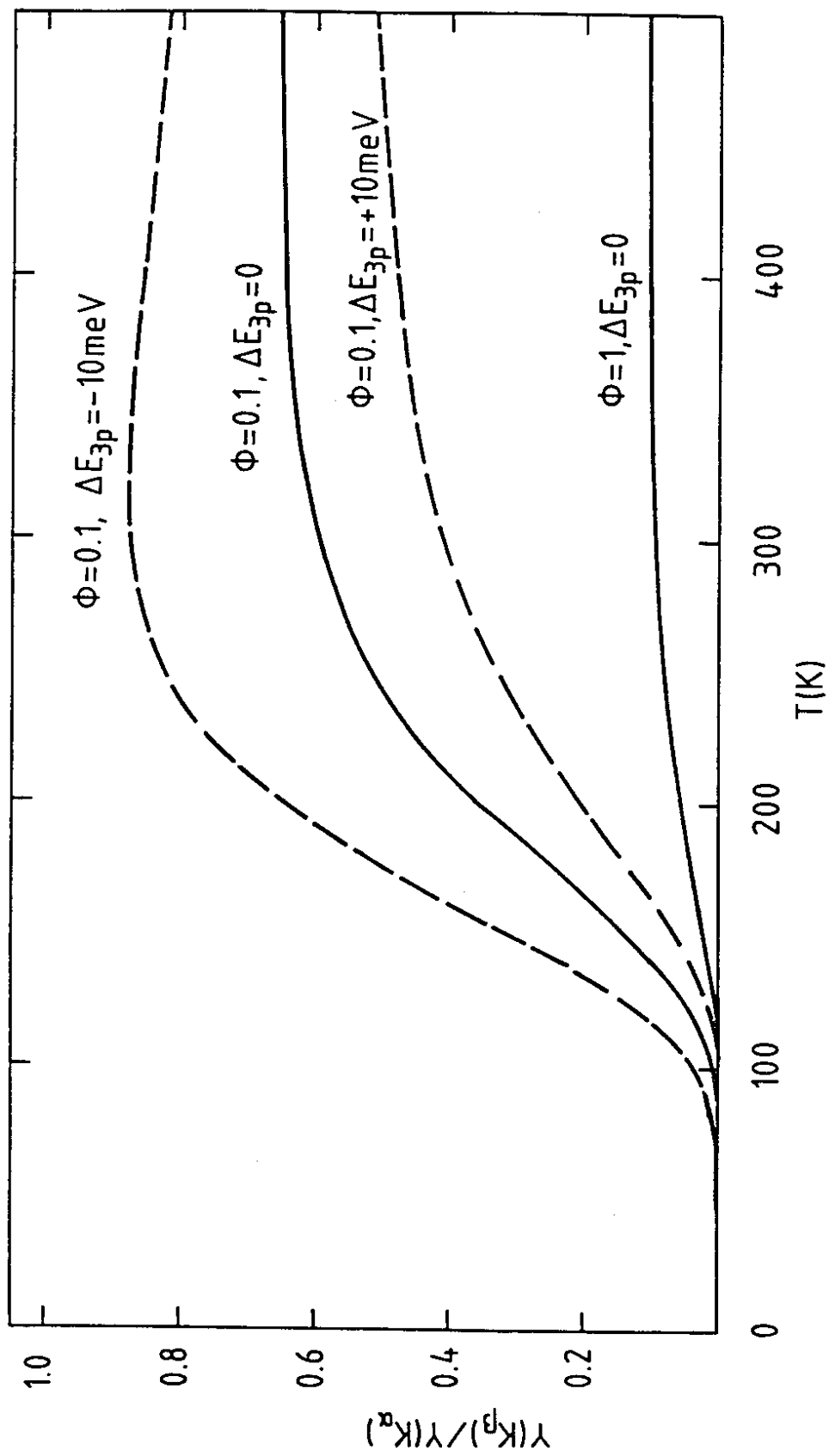


FIG. 4(a).

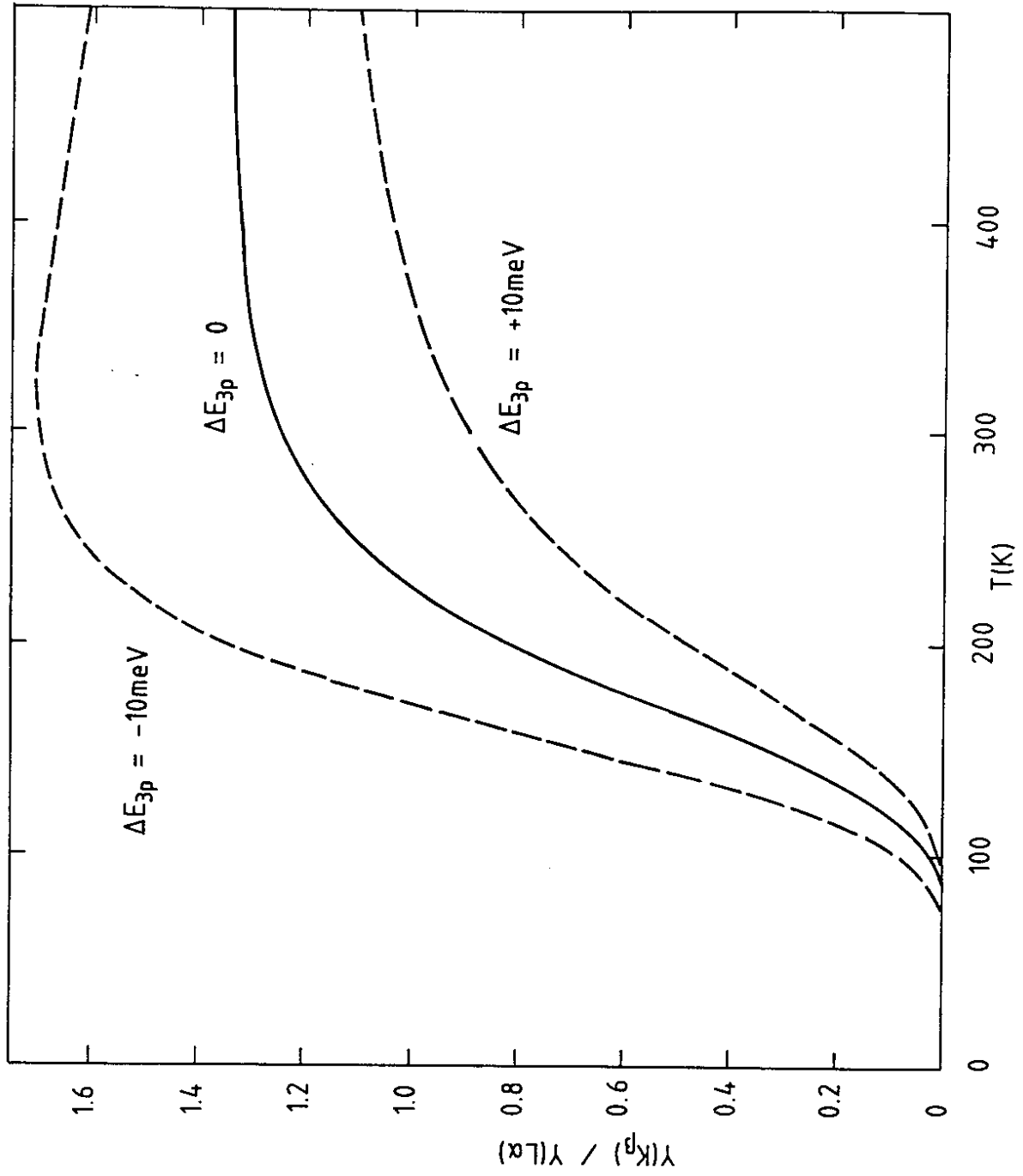


FIG. 4(b).